Journal of Transport Geography 64 (2017) 109–119

Contents lists available at ScienceDirect

Journal of Transport Geography

journal homepage: www.elsevier.com/locate/jtrangeo

Green accessibility: Estimating the environmental costs of network-time prisms for sustainable transportation planning

Ying Song[a,*], Harvey J. Miller[b], Jeff Stempihar[c], Xuesong Zhou[d]

[a] Geography, Environment and Society, University of Minnesota, 414 Social Science Bldg, 267 19th Ave S, Minneapolis, MN 55455, United States
[b] Department of Geography and Center for Urban and Regional Analysis, The Ohio State University, 1036 Derby Hall, 154 North Oval Mall, Columbus, OH 43210, United States
[c] Sustainable Engineering and the Built Environment, Arizona State University, PO Box 873005, Tempe, AZ 85287-3005, United States
[d] Sustainable Engineering and the Built Environment, Arizona State University, College Avenue Commons, Room 474, 660 S. College Ave, Tempe, AZ 85287, United States

ARTICLE INFO

Keywords:
Space-time accessibility
Network-time prism
Emissions

ABSTRACT

Accessibility, or the ease to participate in activities and obtain resources in a given environment, is crucial for evaluating transportation systems. Greater accessibility is often achieved by increasing individuals' potential mobility. However, potential mobility, if realized by motorized modes, can also generate negative environmental impacts such as fossil fuel consumption and greenhouse gas (GHG) emissions. While the negative environmental impacts of greater mobility are acknowledged, there has been a lack of research to validate those impacts using empirical data, especially considering variations in individuals' mobility levels. This paper presents a method for estimating the expected environmental costs of accessibility represented by a network-time prism (NTP). A NTP delimits all accessible locations within a network and the available time for an individual to present at each location given a scheduled trip origin and destination, a time budget and the maximum achievable speeds along network edges. Estimating the expected environmental costs of a NTP involves three steps: (1) semi-Markov techniques to simulate the probabilities to move along network edges at given times; (2) the speed profiles for reachable edges, and (3) a cost function that translates speeds into environmental impacts. We focus on air quality and employ the motor vehicle emission simulator MOVESLite to estimate the CO_2 emissions at both the edge and prism levels. We calibrate and validate the methods for experimental NTPs defined within the Phoenix, AZ, USA road and highway network using vehicles instrumented with GPS-enabled onboard diagnostic devices (OBD). We demonstrate the effectiveness of our method through two scenarios and investigate the impact of changes in mobility levels on the expected CO_2 emissions associated with the experimental NTPs.

1. Introduction

Accessibility describes the ability to participate in activities, obtain resources and opportunities or interact with others within an environment (Cervero, 1996; Geurs and van Wee, 2004; Hansen, 1959; Miller, 2005). There is renewed emphasis on accessibility measurement as part of a shift toward travel demand management and sustainable mobility (Banister, 2008). A widely-used approach is space-time accessibility measures based on the time geographic framework of Hägerstraand (1970). These measures are based on two fundamental concepts: i) the *space-time prism* (STP) that delimits all feasible paths in planar space with respect to time between two anchoring locations and times and ii) the *network-time prism* (NTP) that constrains a STP to a spatial network (Kuijpers and Othman, 2009; Miller, 1991).

Although NTPs are sensitive and effective measures of individual accessibility, they ignore potential negative externalities as defined in Buchanan and Stubblebine (1962). Larger NTPs correspond to higher potential mobility and therefore greater accessibility (Boisjoly and El-Geneidy, 2016; Cetin, 2015; Farber et al., 2013; Kwan, 1998; Lenntorp, 1976; Rigby et al., 2016; Versichele et al., 2014; Widener et al., 2015). But, if this potential mobility is realized via modes such as automobile travel, it will also bring greater costs to the society, including poor air quality (Cetin and Sevik, 2016; Glaeser and Kahn, 2010; Mauzerall et al., 2005), non-renewable resource consumption (Carlsson-Kanyama and Linden, 1999; Chapman, 2007), greenhouse gas (GHG) emissions and global climate change (Rabl et al., 2005; Schafer and Victor, 2000), injuries and fatalities (Dickerson et al., 2007; Kopits and Cropper, 2005) and noise pollution (Janic, 2007; Tompkins et al., 1998).

This paper develops methods for estimating the potential environmental costs associated with NTPs. We focus on fuel consumption and

* Corresponding author.
E-mail addresses: yingsong@umn.edu (Y. Song), miller.81@osu.edu (H.J. Miller), JStempih@asu.edu (J. Stempihar), xzhou74@asu.edu (X. Zhou).

http://dx.doi.org/10.1016/j.jtrangeo.2017.08.008
Received 26 January 2017; Received in revised form 1 July 2017; Accepted 20 August 2017
Available online 09 September 2017
0966-6923/

emissions using vehicle speed as a key parameter (Barth et al., 1996; Franco et al., 2013; Grote et al., 2016). Continuing with our previously developed methods for simulating the expected distribution of visit probabilities within a NTP (Song et al., 2016), we develop methods to estimate the expected speeds within a NTP and procedure to transform visit probabilities and speed profiles into the inputs for an example emission simulator, MOVESLite (Frey and Liu, 2013; Zhou et al., 2015; Vallamsundar et al. 2016) to estimate the expected CO_2 emissions. We illustrate and validate our methods by designing an experimental NTP within the Phoenix, Arizona, USA road and highway network and collecting primary data via vehicles instrumented with GPS-enabled on-board diagnostic devices (OBD). We also provide two example scenarios that investigate the impact of changes in potential mobility on the expected CO_2 emissions associated with a NTP.

This paper also contributes to the development of dynamic, individualistic methods for analyzing mobility, accessibility and environmental costs. Existing methods mainly focus on the marginal cost for additional vehicular flows to the system (e.g. Aziz and Ukkusuri, 2012; Chen and Yang, 2012; Ghali and Smith, 1995; Szeto et al., 2015; Yin and Lawphongpanich, 2006). These models capture the negative impacts of increased mobility, and try to mitigate it through cost-constraint traffic assignment optimization. However, they all focus on the systematic level and the actual/optimized mobility behaviors of individuals. Space-time accessibility based on the NTP can account for individuals' variations in daily schedules (e.g. household responsibilities) by two prism anchors and capture their potential mobility behaviors within various transportation environments (e.g. taking a route different from their regularly one to avoid congestion, pick up a package on their way home). Therefore, planners could utilize measures and estimates developed in this paper to real-world scenario analysis similar to the two example scenarios in this paper.

The rest of the paper is organized as follows. The next section provides background by discussing the NTP, visit probabilities within NTPs, and vehicle emission models. The subsequent section presents the methodology: a general framework to estimate the speed-related cost of a vehicle-specific NTP, three Markovian-based approaches to estimate speed profiles along NTP edges, and methods to derive empirical profiles from vehicle trajectory data. The results section illustrates the procedure, presents results from the model validation, and further illustrates their use through example scenario analysis. The paper concludes with a discussion of future research.

2. Background

2.1. Network-time prisms

A space-time path is a trajectory traced by a moving object in space with respect to time. A *space-time prism* (STP) is an envelope of all possible space-time paths between two locations and times given a maximum speed limit (Hägerstraand, 1970). In transportation studies, we are interested in movements within transportation networks and apply *network-time prism* (NTPs); these are STPs constrained by the geometries, connectivity and speed limits dictated by spatial networks such as roads, trains and other transportation infrastructures (Miller, 1991). NTPs have been recognized as a useful measure of space-time accessibility since it captures individuals' differences in location and scheduling constraints and their available transportation resources (Miller, 1999). NTPs also harmonize well with activity-based methods to model travel demand and analyze sustainable transportation policies (Bhat and Koppelman, 1999; Miller, 2005).

Analytically, the boundaries of the NTP are defined by the earliest arrival time $t_{(x_i,y_i)}^{-}$ and the latest departure time $t_{(x_i,y_i)}^{+}$ at each accessible location (x_i, y_i) (1) and (2):

$$t_{(x_i,y_i)}^{-} = t_{(x_O,y_O)}^{-} + t_{SN}((x_O,y_O),(x_i,y_i)) \quad (1)$$

$$t_{(x_i,y_i)}^{+} = t_{(x_D,y_D)}^{+} - t_{SN}((x_i,y_i),(x_D,y_D)) \quad (2)$$

where (x_O, y_O) and (x_D, y_D) are the origin and destination locations, $t_{(x_O,y_O)}{}^{-}$ is the earliest departure time from the origin, $t_{(x_D,y_D)}{}^{+}$ is the latest arrival time at the destination, and $t_{SN}((x_i,y_i),(x_j,y_j))$ denote the minimum travel time from location (x_i, y_i) to (x_j, y_j) within the network. The location (x_i, y_i) is accessible at time $t \in [t_{(x_O,y_O)}{}^{-}, t_{(x_D,y_D)}{}^{+}]$ if and only if it can be reached from (x_O, y_O) at that time, can arrive at (x_D, y_D) on time, and $t \in [t_{(x_i,y_i)}{}^{-}, t_{(x_i,y_i)}{}^{+}]$.

2.2. Visit probabilities within a NTP

Until recently, researchers have viewed a prism as having homogeneous interiors, with all locations within the prism equally accessible. However, this contradicts intuition: locations near the prism center have greater likelihood of being visited than near the prism boundary, since there are more possible space-time paths near the center. Recent theoretical and empirical studies support this intuition for both STPs and NTPs (Downs and Horner, 2012; Song and Miller, 2014; Winter and Yin, 2010, 2011; Xie and Yan, 2008).

To model visit probabilities within NTPs, Song et al. (2016) model movements along edges within a NTP as a continuous-time semi-Markov process. The methods include transition probabilities describing the likelihood the object will move to each adjacent edge and a holding time density function reflecting the time required (Howard, 2007). These allow us to calibrate the model for a specific spatial network using empirical trajectory data so that the mobility level of the network can be captured in the simulated visit probabilities. To validate the methods, Song et al. (2016) derive empirical visit probabilities using trajectory data collected by a commercial ridesharing service in Manhattan, NYC, USA, and compare them to the simulated probabilities. Both visual and quantitative comparisons indicate good fit.

2.3. Modeling vehicle energy consumption and emissions

Traditional approaches model the environmental impacts of mobility at the aggregate-level using methods such as the four-step travel demand model as a basis. However, aggregate methods are not well-suited for policy questions surrounding travel demand management and sustainable mobility provision (Banister, 2008; Bhat and Koppelman, 1999). Recently, microscopic models (e.g. TRANSIMS, NETSIM, MOVES, EMFA) have incorporated traffic simulation models to generate emission estimates. They consider individual vehicles and examine how their costs change over time and with respect to infrastructure and policy changes.

These fuel consumption and emission models relate various input factors contributing to the estimates; these include: (1) *travel-related factors* (e.g. distance travelled, speed) (An and Ross, 1993; Humphrey, 1996); (2) *highway network characteristics and conditions* (e.g. geometries, road surface conditions) (Baker, 1994); (3) *vehicle-related factors* (e.g. weight, engine type, age) (Murrel, 1980); and (4) *other factors* (e.g. ambient temperature, wind speeds) (Ahn, 1998).

This paper focuses on the speed-related cost of individuals' potential mobility. We use MOVESLite, a simplified version of the EPA's *Motor Vehicle Emission Simulator (MOVES)* model, because it allows us to estimate energy consumption and emissions given speed profiles of a vehicle with a specific type as input (Zhou et al., 2015, Vallamsundar et al. 2016). Hence, our methods provide NTPs' emission estimates for a given vehicle type including passenger car, passenger truck, light commercial truck, single unit short haul truck and long haul truck.

3. Methodology

3.1. NTP expected cost model

Estimating the expected speed-related NTP cost requires three

components: i) the distribution of visit probabilities; ii) the possible speeds along edges at different times; and iii) a function that translates speeds into costs such as energy consumption and GHG emissions. We outline the general model and discuss details below.

Given a transportation network represented by a graph of directed edges, we simulate movements among vertices and generate visit probabilities within the NTP using semi-Markov techniques (Song et al. 2016). First, we use trajectory data collected in Phoenix, AZ, USA to calibrate the holding time density function $h(\tau)$. This describes the probability that movements from vertex $v_i{:}(x_i,y_i)$ to vertex $v_j{:}(x_j,y_j)$ will take an extra $\tau=(t-t_{min})/t_{min}$ amount of time beyond the minimum travel time t_{min}, where $t_{min}=t_{SN}((x_i,y_i),(x_j,y_j))$. We then simulate the probabilities that the object is moving from v_i to v_j along edge e_{ij} at time $t\in[t_{(x_o,y_O)^-},t_{(x_D,y_D)^+}]$, denoted as $P(v_i\rightarrow v_j{:}\,e_{ij},t)$. After that, we use the same $h(\tau)$ to derive speed profiles along edges, denoted as $P(s\,|\,(v_i\rightarrow v_j{:}\,e_{ij},t))$, where s is a speed within the speed limit along the edge e_{ij}. Finally, the probability of moving at speed s from v_i to v_j along e_{ij} at time t is given as the product of visit probabilities and speed distributions:

$$P(v_i\rightarrow v_j{:}\,e_{ij},s,t)=P(s\mid(v_i\rightarrow v_j{:}\,e_{ij},t))\times P(v_i\rightarrow v_j{:}\,e_{ij},t) \tag{3}$$

Given an array of vehicle specific attributes A_{car}, an array of road physical conditions $A_{v_i\rightarrow v_j:e_{ij}}$, and a function $C(s\,|\,(A_{car},A_{v_i\rightarrow v_j:e_{ij}}))$ that translates speed s into some environmental cost, the expected environmental cost of a NTP edge at time t is:

$$C((v_i\rightarrow v_j{:}\,e_{ij},s,t)\,|(A_{car},A_{v_i\rightarrow v_j:e_{ij}}))=P(v_i\rightarrow v_j{:}\,e_{ij},s,t)\times C(s\mid(A_{car},A_{v_i\rightarrow v_j:e_{ij}})) \tag{4}$$

Summing over all edges and times within a NTP provides an estimate of its overall cost.

3.2. Simulating the speed distribution within a NTP

This section discusses three methods to derive speed distributions along directed edges within a NTP, $P(s\,|\,(v_i\rightarrow v_j:e_{ij},t))$ using the same holding time density function $h(\tau)$ calibrated and applied to simulate the NTP's visit probabilities.

3.2.1. Method 1: constant speed based on mean arrival and departure times

We start with the assumption that the vehicle will move with constant speed along edge e_{ij} after leaving v_i at mean arrival time from the origin to v_i and before arriving at v_j at mean departure time from v_j to the destination. Given the mean of $h(\tau)$ as $\mu(\tau)$, the mean arrival time at v_i and the mean departure time from v_j are:

$$\mu_{e_{ij}}(t_{v_i})=\mu(\tau_{v_i})\times(t^-_{v_i}-t^-_{(x_O,y_O)})+t^-_{(x_O,y_O)} \tag{5}$$

$$\mu_{e_{ij}}(t_{v_j})=t^+_{(x_D,y_D)}-\mu(\tau_{v_j})\times(t^+_{(x_D,y_D)}-t^+_{v_j}) \tag{6}$$

where τ_{v_i} is the extra time spent to reach v_i related to the minimum time from origin to v_i, and τ_{v_j} is the extra available time at v_j related to the minimum time from v_j to destination. Given the length l_{ij} and maximum achievable speed s_{ij}, the expected speed along e_{ij} is:

$$\mu_{e_{ij}}(s)=\frac{l_{ij}}{\mu_{e_{ij}}(t_{v_i})-\mu_{e_{ij}}(t_{v_j})} \tag{7}$$

3.2.2. Method 2: constant speed based on truncated arrival and departure times

We modify the first method and adopt the truncated form of $h(\tau)$ to limit the distribution domain within the feasible arrival and departure times (Johnson et al., 1996). The lower and upper bounds at the two end vertices v_i and v_j are:

$$(LB_{v_i},UB_{v_i})=\left(0,\frac{t^+_{v_j}-t_{SN}(v_i,v_j)-t^-_{v_i}}{t^-_{v_i}-t^-_{(x_O,y_O)}}\right) \tag{8}$$

$$(LB_{v_j},UB_{v_j})=\left(0,\frac{t^+_{v_j}-t_{SN}(v_i,v_j)-t^-_{v_i}}{t^+_{(x_D,y_D)}-t^+_{v_j}}\right) \tag{9}$$

Given the cumulative density function of $h(\tau)$ as $H(\tau)$, the truncated mean arrival and departure times are:

$$\mu^{Trun}_{e_{ij}}(t_{v_i})=\frac{\int_{t^-_{v_i}}^{t^+_{v_j}-t_{SN}(v_iv_j)}h\left(\frac{t-t^-_{v_i}}{t^-_{v_i}-t^-_{(x_Oy_O)}}\right)dt}{H(UB_{v_i})-H(LB_{v_i})} \tag{10}$$

$$\mu^{Trun}_{e_{ij}}(t_{v_j})=\frac{\int_{t_{SN}(v_iv_j)+t^-_{v_i}}^{t^+_{v_j}}h\left(\frac{t^+_{v_j}-t}{t^+_{(x_Dy_D)}-t^+_{v_j}}\right)dt}{H(UB_{v_j})-H(LB_{v_j})} \tag{11}$$

Hence, the expected speed is along the edge e_{ij}:

$$\mu^{Trun}_{e_{ij}}(s)=\frac{l_{ij}}{\mu^{Trun}_{e_{ij}}(t_{v_i})-\mu^{Trun}_{e_{ij}}(t_{v_j})} \tag{12}$$

3.2.3. Method 3: travel time based on the holding time function $h(\tau)$

We apply the same $h(\tau)$ for movements along edges between adjacent vertices. Compared with the previous two methods, this method assigns probabilities to all feasible speeds in addition to the mean speed. Given the minimum time required along e_{ij} as $t_{SN}(v_i,v_j)$, the extra time τ_{ij} related to $t_{SN}(v_i,v_j)$ spent for the movement $(v_i\rightarrow v_j:e_{ij})$ should satisfy $h(\tau_{ij})$, with mean speed as:

$$P\mu_{e_{ij}}(s)=\frac{l_{ij}}{(\mu(\tau_{ij})+1)\times t_{SN}(v_i,v_j)} \tag{13}$$

3.3. Deriving empirical speed profiles

To validate the simulated speed profiles, we develop methods to derive empirical speed profiles from vehicle trajectories collected within a real-world NTP. Each trajectory is usually stored as an ordered series of locations and speeds at recorded time, denoted as $Trj^{id}{:}\{t_k,(x_k,y_k),s_k\}^{id}$, where id is its identifier, t_k is a recorded time with index $k=0,1,2,\ldots$, and (x_k,y_k) and s_k are the coordinates and speed recorded at t_k. The original time series $\{t_k\}^{id}$ usually include clock times and dates, so we calculate the relative time series $\{\hat{t}_k=t_k-t^-_{(x_O,y_O)}\}^{id}$ to the prism departure time $t^-_{(x_O,y_O)}$ of each day. This allows us to define a NTP using budgeted time $(t_{(x_D,y_D)^+}-t_{(x_o,y_O)^-})$, and use trajectories collected at different days. We also map-match each trajectory to the spatial network as a route Rt^{id}, and linear-referenced each recorded location along that route. Therefore, each pair of recorded coordinates (x_k,y_k) is map-matched to a directed edge e_{ij} and stored as a referenced location along the route $lr_k^{Rt}=l_{SN}^{Rt}((x_O,y_O),(x_k,y_k))$. A sample trajectory can be represented as $Rt^{id}{:}\{(\hat{t}_k,lr_k^{Rt},s_k)\}^{id}$.

For fine-scale trajectory data, it is reasonable to assume a constant acceleration between two consecutive locations $(\hat{t}_k,\ lr_k^{Rt},s_k)$ and $(\hat{t}_{k+1},lr_{k+1}^{Rt},s_{k+1})$, and model the movement:

$$lr_{k+1}^{Rt}=lr_k^{Rt}+\left(s_k\times\Delta t_{k,k+1}+\frac{a_{k,k+1}\times\Delta t_{k,k+1}{}^2}{2}\right)\times(1+\varepsilon_{k,k+1}) \tag{14}$$

$$s_{k+1}=s_k+a_{k,k+1}\times\Delta t_{k,k+1} \tag{15}$$

$$\Delta t_{k,k+1}=\hat{t}_{k+1}-\hat{t}_k \tag{16}$$

where $\varepsilon_{k,k+1}$ is a factor considering the errors during data collection

and map-matching process. For any $\hat{t} \in [0, (t_D - t_O)]$, we calculate the instant speed $s^{id}(\hat{t})$ and referenced location $lr^{id}(\hat{t})$ based on its two direct neighbors $(\hat{t}_n,\ lr_n^{Rt}, s_n)$ and $(\hat{t}_{n+1}, lr_{n+1}^{Rt}, s_{n+1})$:

$$s^{id}(\hat{t}) = s_n + \frac{s_{n+1} - s_n}{\hat{t}_{n+1} - \hat{t}_n} \times (\hat{t} - \hat{t}_n),\ \hat{t} \in [\hat{t}_n, \hat{t}_{n+1}] \tag{17}$$

$$lr^{id}(\hat{t}) = lr_n^{Rt} + [(s_n + s^{id}(\hat{t})) \times (\hat{t} - \hat{t}_n)] \times \frac{lr_{n+1}^{Rt} - lr_n^{Rt}}{(s_{n+1} - s_n) \times (\hat{t}_{n+1} - \hat{t}_n)} \tag{18}$$

Given the referenced location $lr^{id}(\hat{t})$, we use the linear-reference method again and get the corresponding directed edge $e^{id}(\hat{t})$. The empirical distribution of visit probabilities and speed profiles at $\hat{t} \in [0, (t_D - t_O)]$, are derived based on the result set $Emp(\hat{t})$: $\{s^{id}(\hat{t}), e^{id}(\hat{t})\}$ for N recorded trajectories $\{Rt^{id}\}$:

$$P^{Emp}(v_i \to v_j;\ e_{ij}\hat{t}) = \begin{cases} 0, & e_{ij} \notin \{e^{id}(\hat{t})\} \\ Freq(e_{ij})/N, & e_{ij} \in \{e^{id}(\hat{t})\} \end{cases} \tag{19}$$

where $Freq(e_{ij})$ is the total occurrence of e_{ij} in set $\{e^{id}(\hat{t})\}$. We compare it to the simulated distribution $P^{Sim}(v_i \to v_j;\ e_{ij}, \hat{t})$ using the root mean square error (RMSE) for all accessible edges at time $\hat{t}$.

We also compare empirical and simulated speed profiles to determine the method with the best performance. We first find the corresponding speeds from $Emp(\hat{t})$: $\{s^{id}(\hat{t}), e^{id}(\hat{t})\}$ for each accessible edge at time $\hat{t}$. Since edges within a NTP do not have the same speed limits and visit probabilities, we then normalize the simulated and empirical speed profiles of each edge by its speed limit and assign a weight to it based on its simulated and empirical visit probability at time $\hat{t}$ when we calculate the RMSE.

3.4. NTP speed profiles for MOVESLite

The MOVESLite estimates energy consumption and emissions by deriving the vehicle specific power (VSP): the second-by-second vehicle power demand considering kinetic energy, rolling resistance, aerodynamic drag, and gravity (EPA, 2012):

$$VSP = \frac{(A_{TR,v} \times v_t) + (B_{RR,v} \times {v_t}^2) + (C_{AD,v} \times {v_t}^3) + \{M_v \times v_t \times (a_t + gr_t)\}}{M} \tag{20}$$

where $A_{TR,v}$, $B_{RR,v}$, $C_{AD,v}$ and M_v are tire rolling resistance, rotational resistance, aerodynamic drag coefficient and source mass factor mass for vehicle type v, v_t and a_t are the instantaneous vehicle speed and acceleration at time t, and r_t is road grade. For passenger cars:

$$VSP = \frac{0.156461 \times v_t + 0.00200193 \times {v_t}^2 + 0.000492646 \times {v_t}^3 + 1.4788 \times v_t \times a_t}{1.4788} \tag{21}$$

The acceleration is estimated as the difference between the speeds during two consecutive seconds, which is consistent with our method to derive empirical speed profile (Eq. (17)):

$$a_t = a_{t-1,t} = s_t - s_{t-1} \tag{22}$$

Then, MOVESLite uses the VSP-to-Operating Mode conversion table to obtain average emission rates stratified by vehicle type, age and operating mode. Table 1 shows an example for passenger cars' gasoline consumption and CO_2 emissions. Given the vehicle type and the speed profile along its moving route, we can obtain emission measures of that route (including energy, CO_2, NOx, CO, hydrocarbons) (Frey and Liu, 2013). The estimations generated by MOVESLite correspond well with the MOVES model with a lower computational cost.

Considering the general mechanism of MOVESLite, we simulate speed profiles for an NTP at both edge and prism levels. Since the original profiles as $P(v_i \to v_j : e_{ij}, s, t)$ do not satisfy the input formats for MOVESLite, we create 11 bins for possible speed and VSP combinations, each corresponding to an operation mode in the VSP-to-Operating Mode conversion table. We then aggregate speed profiles of edge and prism into bins and use it as input for MOVESLite.

4. Implementation and study design

We implement the methodology using the programming language Python and its four supported modules: i) Numpy for large-size arrays, ii) Scipy for statistic functions, iii) Sympy for solving high-order equations, and iv) ArcPy (a site package provided with ESRI ArcGIS software) for conducting network analysis and visualizing results. We develop and manage functions, classes, and modules using PyCharm, an intelligent and customizable Python IDE.

The evaluation of our methods uses Phoenix, Arizona, USA as the study area because of the availability of secondary data from a commercial ridesharing service. The network dataset is the North American Detailed Streets (NADS) downloadable from ESRI online data resources. We use the free-flow speeds along highways and arterial streets provided by local government agencies in addition to the NADS to derive the maximum speeds along edges.

We evaluate the methods by analyzing empirical data for experimental NTPs. First, we calibrate the holding time function using secondary data available in the study area, and use it to design driving routes for primary data collection that can reflect the estimated visit probability distribution for a specified NTP. Second, we employed trained research assistants to drive these routes using cars instrumented with GPS receivers and i2D onboard diagnostic devices (OBDs) that capture second-by-second locations, speeds, and engine performance parameters. We use OBDs due to the unavailability of tailpipe emissions monitors; additional research could continue this evaluation using other technology. Finally, we use the primary data to generate empirical visit probabilities, speed profiles and expected CO_2, and compare it to our model estimates.

4.1. Calibrating the holding time density function using secondary data

We calibrate the function $h(\tau)$ for Phoenix area using trajectory data provided by a commercial ridesharing service. We selected trajectories with recorded time of approximately 25 min to provide a sufficient trip length for fuel consumption and emissions (EPA, 2012). We eliminate trajectories with missing data along the route. The final dataset consists of 159 trajectories map-matched to the NADS networks.

Since these trajectories do not share the same origin and destination, we use the quickest path time, $\min(t_{OD})$, as the base to normalize the recorded trip time, $\text{rec}(t_{route})$; the normalized extra time is hence: $\tau = (\text{rec}(t_{route}) - \min(t_{OD}))/\min(t_{OD})$. We use the programing language R and maximum likelihood method to find the best fitted distribution to these normalized extra times. The Log-normal distribution has the best fit:

$$h(\tau) = \frac{1}{\tau\sigma\sqrt{2\pi}} e^{-\frac{(ln\tau - \mu)^2}{2\sigma^2}} \tag{23}$$

where $\mu \approx 3.6527$ is the log of mean, $\sigma \approx 0.7134$ is the log of standard deviation, and standard errors for μ and σ between fitted and actual distributions are 0.0566 and 0.0400, respectively.

4.2. Primary data collection

We design an empirical NTP in Phoenix area using 25 min as the time budget. The origin and destination anchors are a parking lot at Arizona State University, Tempe campus (at the crossing of S Rural Rd. and E 6th St., Tempe, AZ) and a parking lot in Scottsdale Fashion Square Mall (at 4569–4605 N 68th St., Scottsdale, AZ), respectively.

Based on the calibrated mobility level in Phoenix area, we simulate visit probabilities within the NTP (Fig. 1), and select routes to reflect

Table 1
Operation mode and the corresponding mean CO_2.

Operating mode ID	Speed (mph)	Vehicle specific power, VSP_t (kW/metric ton)	Corresponding max speed (m/s)	Corresponding mean base rate for CO_2 (g/s)	Corresponding mean base rate for gasoline (g/s)
11	$1 \le v_t < 25$	$VSP_t < 0$	0.4470	1.2255	0.4419
21	$25 \le v_t < 50$	$VSP < 0$	11.1760	1.6672	0.6011
22		$0 \le VSP_t < 3$	14.9569	1.8978	0.6843
23		$3 \le VSP_t < 6$	21.1581	2.3114	0.8334
24		$6 \le VSP_t < 9$	25.3756	2.9653	1.0692
33	$50 \le v_t$	$VSP < 6$	22.3520	2.3753	0.8564
35		$6 \le VSP_t < 12$	28.6732	3.8088	1.3733
37		$12 \le VSP_t < 18$	33.8099	4.9616	1.7889
38		$18 \le VSP_t < 24$	37.8449	6.4697	2.3327
39		$24 \le VSP_t < 30$	41.2236	8.6175	3.1071
40		$30 \le VSP_t$	–	10.9852	3.9608

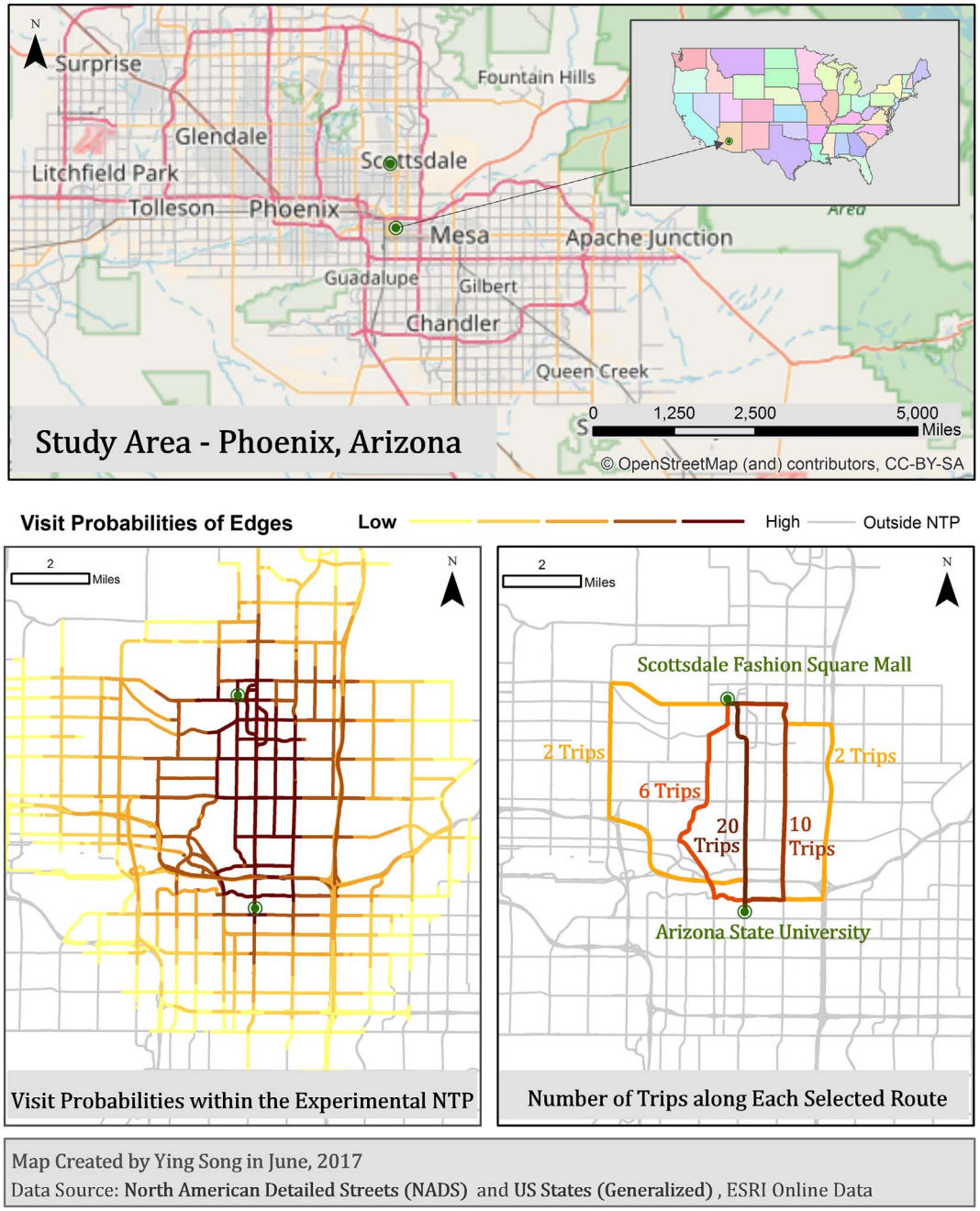

Fig. 1. Visit probabilities and designated routes within the experimental NTP.

the distribution. Given the limited number of trips available for primary data collection, we swapped the origin and destination anchors and define a second NTP, which has a similar visit probabilities distribution as the first NTP and can use the same routes with opposite directions. Fig. 1 shows the selected routes and the number of trips along each route. Based on local knowledge, we restrict these routes to highways and arterial roads rather than using residential streets considering realistic driving behaviors.

We collected primary data using vehicles instrumented with GPS receivers and i2D onboard diagnostics (OBD). The data was transmitted in real-time to cloud-based storage via mobile network connection. We employed research assistants to drive the instrumented vehicles along these routes. For safety purposes, each trip also included a second research assistant who has studied the routes before data collection and was responsible for navigation. We also explained the purpose of the data collection to the research assistants and provided them with detailed driving instructions before the trips. We instructed each team to drive two round trips (4 trips) between Arizona State University and Scottsdale Fashion Square Mall. Trips were distributed in a manner so that each team could drive along different routes.

The original data includes 68 fields per record. We selected 8 fields for empirical analysis: *route id*, *trip id*, *recorded seconds*, *latitude, longitude*, *instant speed, and gasoline consumption*. We create an ESRI point shapefile based on latitudes and longitudes, and map-matched these points to NADS network. We excluded two trips that do not fulfill the data quality requirements due to the device deficiency, and created an empirical database with 38 trips.

5. Results

5.1. Holding time function and NTP visit probabilities

We first update the holding function using the primary data. Fig. 2 shows that the best fit is the lognormal distribution with $\mu \approx 3.89$ and $\sigma \approx 0.94$, with the standard errors for μ and σ as 0.15 and 0.11 respectively. We compare the simulated and empirical visit probabilities and the RMSE at selected times for the two NTPs indicates good fit ($< 1\%$ for most selected time). This indicates that the designed routes can provide sample trajectories within the NTP that well fit the theoretical distribution of visit probabilities and therefore can well represent the entire population of possible trajectories within the NTP.

5.2. NTP speed distribution

We estimate NTP speed distributions using the updated $h(\tau)$. Considering the different speed limits along edges, we visualize the ratio of the derived speeds to the maximum speeds. If the derived speed is larger than the maximum speed along an edge, we assign null value to it.

Fig. 3(a) shows the speed profile derived from the mean arrival and departure times. The yellow area is the NTP's spatial footprint, or potential network area (PNA), consisting of 46,786 road segments. Since the NTP time budget is not considered in this method, a substantial portion of the arrival and departure times violate NTP constraints. Fig. 3(b) shows the speed distributions using the truncated method. It shows a large region of slow speeds, and only a few edges close to PNA boundary has higher moving speeds. Fig. 3(c) illustrates results based directly on $h(\tau)$. Similar to the truncated method, the mean speeds never exceed the maximum achievable speeds. The results from the third method appear more plausible. To confirm this, we calculate the RMSE between the theoretical mean speeds and the empirical speeds based on the primary data. Since the speed limits along edges vary, we normalize the recorded speeds by the speed limit for each edge. The RMSEs for the three methods are 2.57% based on mean arrival and departure times, 2.45% based on truncated mean and departure times, and 0.70% based on h(τ). This confirms that the third method has the best performance; therefore, we use this method to estimate NTP costs.

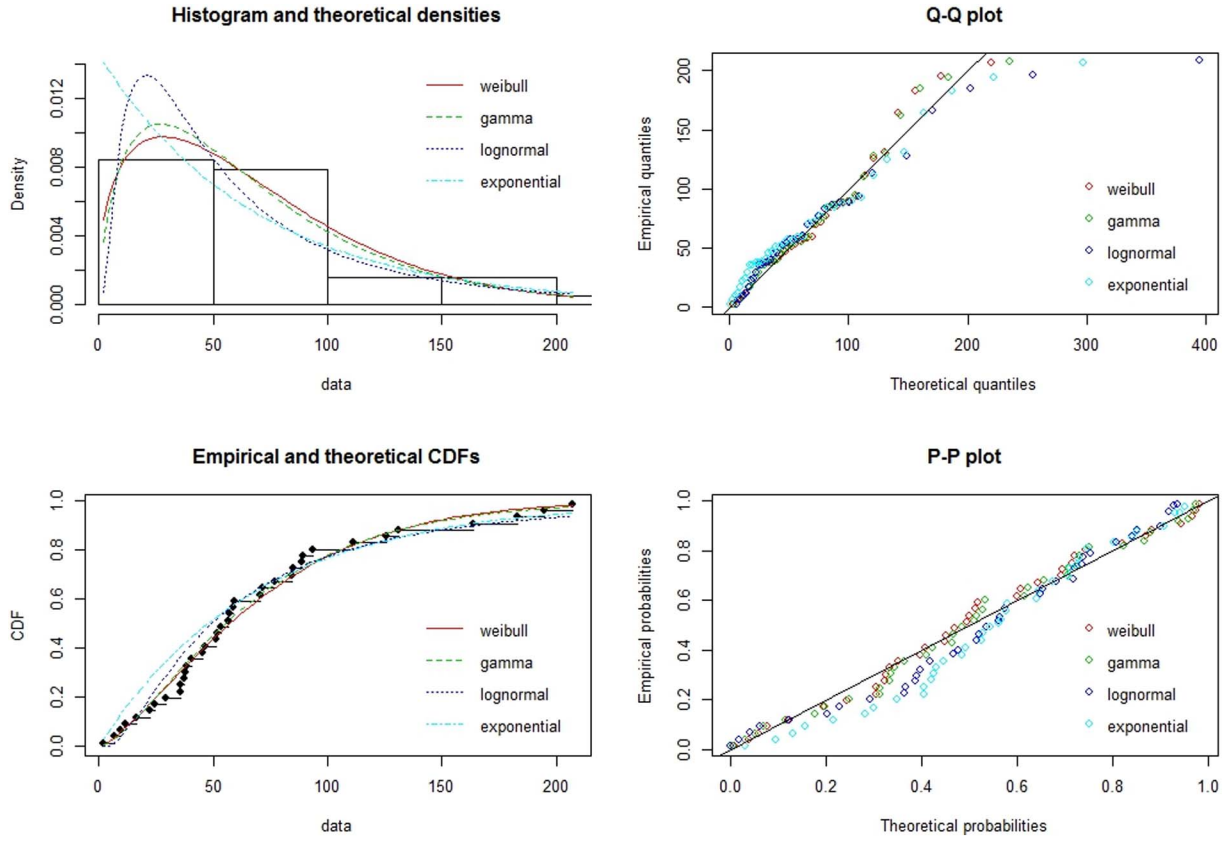

Fig. 2. Empirical and fitted distribution of extra time with respect to minimum time.

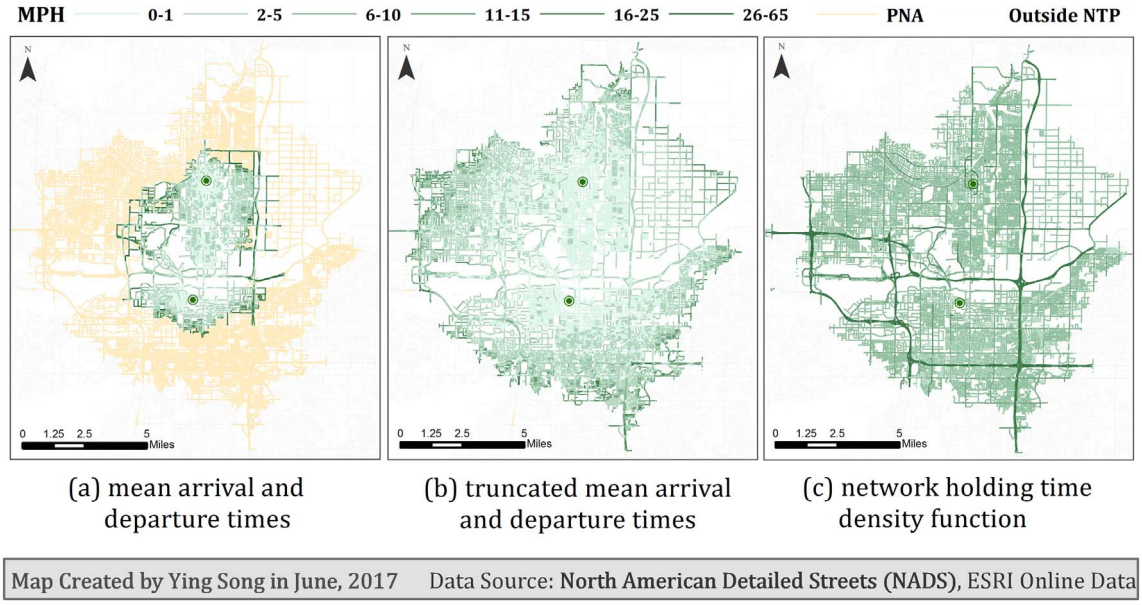

Fig. 3. Mean speed distribution derived based on three methods.

5.3. NTP expected energy consumption and CO_2 emissions

Given visit probabilities and speed profiles of edges, we estimate the fuel consumption and CO_2 emissions at both edge and NTP levels. First, we calculate the expected speeds along edges using Eq. (13) with expected acceleration as zero. Then, we refer to Table 1 for the corresponding operation modes and the mean base rates for fuel consumption and CO_2 emission of passenger cars. Finally, we multiply the expected costs along edges with their visit probabilities at selected times to get the spatial distribution of expected costs.

We estimate the fuel consumption along each edge and compare it to the empirical one derived from our primary data. To eliminate the impacts of visit probabilities on the comparison results, we do not combine edges' expected fuel consumption with the visit probabilities. Fig. 4 shows the differences (g/s) for all edges: the estimated costs slightly biased toward larger than the empirical costs. The RMSE for all edges is 0.34, indicating a good fit overall for all edges.

We continue to estimate and visualize CO_2 emissions at both edge level. Fig. 5 shows the distributions of expected CO_2 emissions at select times for the empirical NTP from Arizona State University to Scottsdale Fashion Square mall. Although the distributions are largely affected by edge visit probabilities, due to the variations of speed profiles, edges with higher speed limits result in higher expected emissions. We also estimate CO_2 emissions at prism level, Table 2 shows the estimations at selected times for two empirical NTPs. Despite similar overall emissions across time, a larger accessible area results in a higher cost, which is consistent with our intuition that greater mobility may result in larger environment costs.

5.4. Scenario analysis: NTP changes and CO_2 emissions

The methods in this paper can be used to assess the environmental costs of anticipated/proposed changes in space-time accessibility. To illustrate this, we created two scenarios to examine the impacts of changes on the expected benefits and costs of accessibility. In the first scenario, speed limits along network edges were increased/decreased by 5 MPH. Essentially, this change affects the size of the NTP. Table 3 shows that the potential network path area (NPA) become larger as speed limits increase, which indicates that the network with higher speed limits provided greater potential mobility. However, we expect an approximate 3% increase in CO_2 emissions for a 25-minute one-way trip. In comparison, if speed limits were reduced by 5 MPH, reasonable levels of accessibility could be maintained while reducing the expected emissions by over 10% for a 25-minute one-way trip.

A second scenario considered differences in mobility levels within the NTP due to factors such as adding or reducing lanes, changes in travel demand, or other changes affecting the travel time delays. We adjusted the dispersion parameters in the holding time density function (Eq. (23)) in order to add and drop the expected (mean) time delayed along each edge by 20%. Adding and dropping the time delays

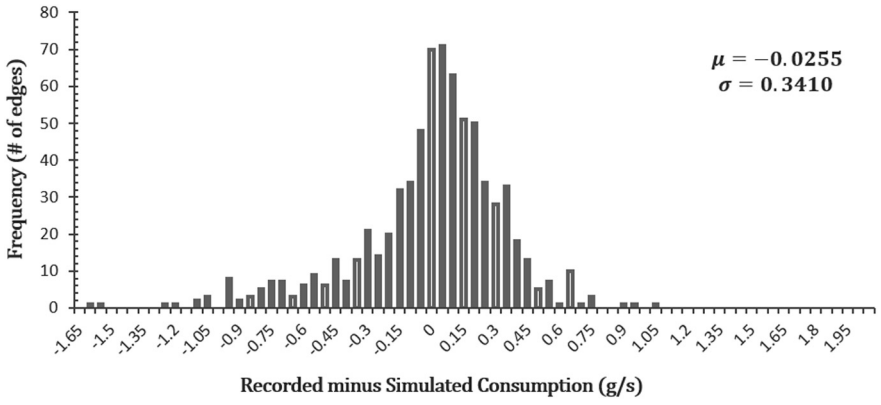

Fig. 4. Difference between recorded and simulated energy consumption for all edges.

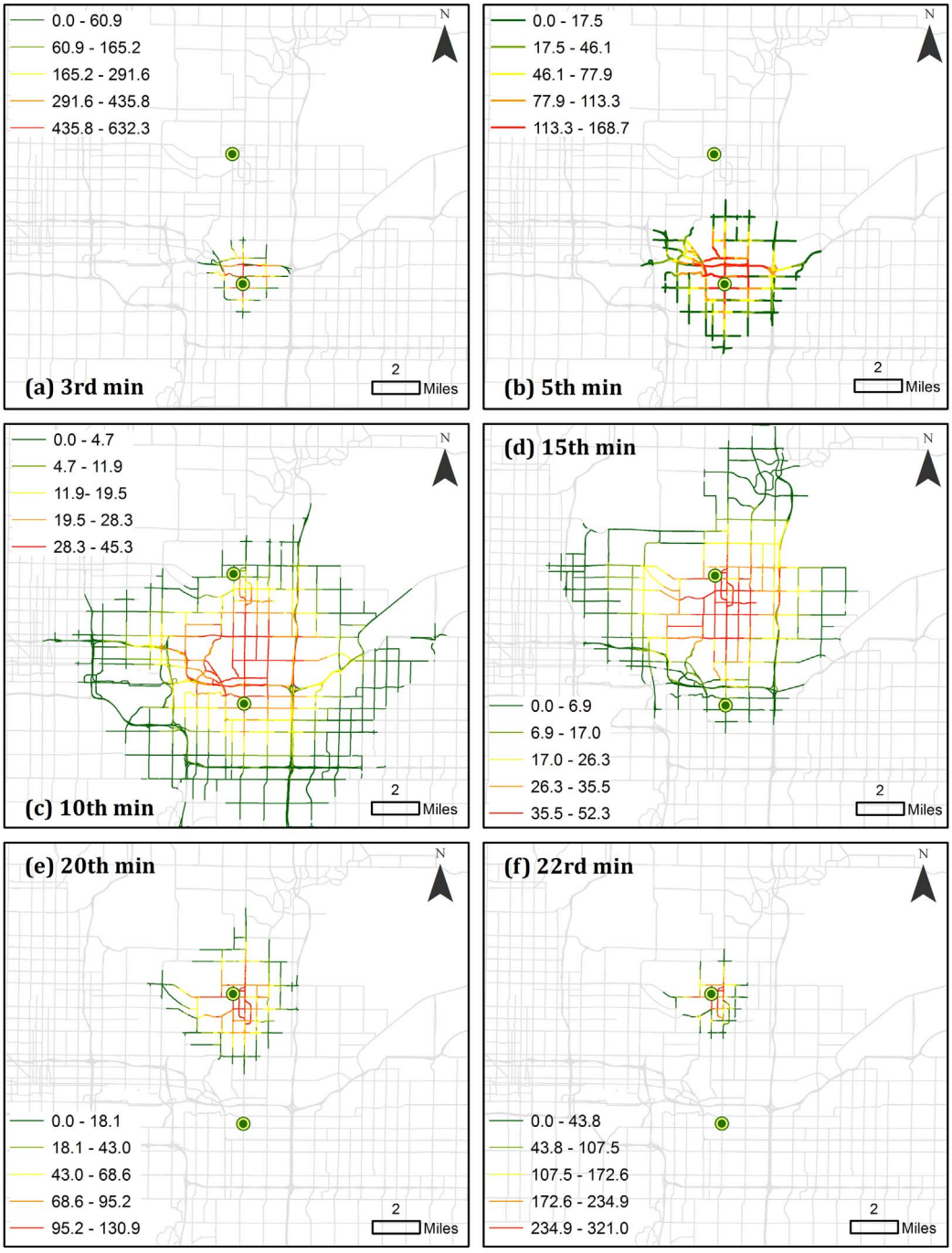

Fig. 5. Distribution of expected CO_2 emissions (mg/s) at selected times within the NTP.

correspond to a decrease and increase in mobility levels, respectively. The changes in the mobility level affect the distribution of visit probabilities and expected speeds within the NTP, and therefore the spatial distribution of expected CO_2 emissions. With less mean time delays, we expect even higher visit probabilities with larger expected (mean) speeds toward the prism center, which lead to even more concentrated CO_2 emissions toward the prism center and possible worse air quality along these edges and surroundings (see Fig. 6). Besides, Table 4 shows that the total emission increases slightly when we have 20% fewer expected time delays. This is largely because a higher mobility level also ties with higher expected speeds along edges and more expected CO_2 emissions.

6. Conclusion

This paper develops methods for estimating environmental costs associated with network time prism (NTP) measures of space-time accessibility. Given origin and destination anchors, time budget for travel, maximum achievable speeds within a transportation network and a vehicle type, our methods estimate both the potential mobility afforded by a NTP along with its expected speed-related environmental costs such as energy consumption and emissions. We develop a general framework using three successive steps: i) simulating the probability that an object is moving along an edge among all accessible edges within a NTP; ii) calculating the probability that this movement has an instant

Table 2
Expected total NTP CO_2 emissions (g/s) at selected times.

(a) From Arizona State University to Scottsdale Fashion Square Mall

Time	1st min	3rd min	5th min	10th min	15th min	20th min	22nd min	24th min
CO_2	3.54	3.58	3.65	3.68	3.65	3.66	3.64	3.57

(b) From Scottsdale Fashion Square Mall to Arizona State University

Time	1st min	3rd min	5th min	10th min	15th min	20th min	22nd min	24th min
CO_2	3.61	3.65	3.66	3.66	3.68	3.64	3.55	3.54

Table 3
NPA size (km) and expected CO_2 emissions (g) under different speed limits.

Direction	Potential network path area (km)			CO_2 emissions (g)		
	Baseline	Max speed + 5 MPH	Max speed − 5 MPH	Baseline	Max speed + 5 MPH	Max speed − 5 MPH
ASU to Scottsdale Mall	1782.48	2291.75 (+28.57%)	1440.30 (−19.20%)	6048.42	6231.88 (+3.03%)	5391.32 (−10.86%)
Scottsdale Mall to ASU	1800.92	2315.29 (+28.56%)	1466.61 (−10.86%)	6045.53	6231.23 (+3.07%)	5398.66 (−10.70%)

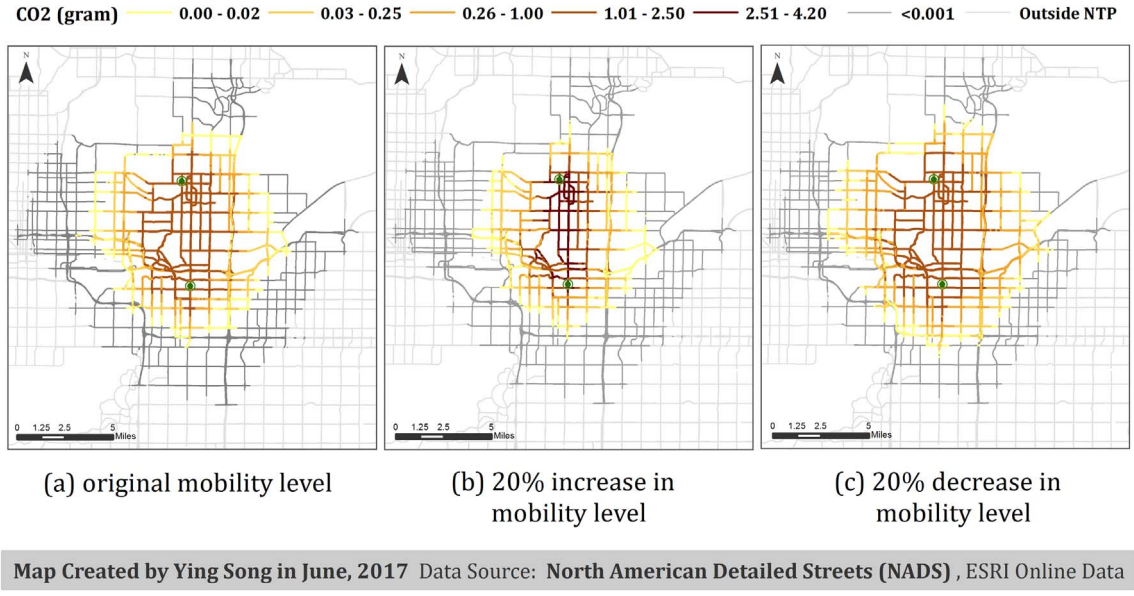

Fig. 6. Edge Total Expected CO_2 Emissions under Different NTP Mobility Levels.

Table 4
Expected CO_2 emissions for a 25-min one-way trip under various mobility levels.

Direction	Baseline total NTP CO_2 emissions (g)	20% decrease in expected delays	20% increase in expected delays
From ASU to Scottsdale Mall	6048.42	6218.54 (+2.03%)	5249.69 (−13.21%)
From Scottsdale Mall to ASU	6045.53	6218.71 (+2.86%)	5249.83 (−13.16%)

speed among all feasible speeds along that edge, and; iii) integrating the distribution of visit probabilities and edge speeds to derive the NTP speed distribution as input for vehicle energy consumption and emission models (e.g. MOVELite) to estimate specific types of costs (e.g. GHG emissions). We adopt the Markovian techniques developed in our previous study to simulate the visit probabilities, develop methods to simulate speed profiles along edges within the NTP, and translate expected speeds into inputs for the selected cost function. We validate our methods using secondary and primary data in Phoenix, Arizona, USA, find good fit and illustrate our method at the edge and overall prism levels.

A next step is to continue validation of the methods by getting direct tailpipe emissions measurements and high quality recorded speeds. The methods developed in this paper can also be extended by considering vehicle acceleration, another speed-related parameter that influences fuel consumption and vehicle emissions. There are tractable methods for capturing acceleration and deceleration constraints within NTPs (Kuijpers et al., 2011), which should be extended to prism interior properties such as visit probabilities and speed distributions, also adding to the analytical foundation for time geography (Winter and Yin, 2010, 2011). The methods can also be extended to account for possible activities between two prism anchors. The definition of such NTPs requires the distribution of such activity locations and their

available times, and the visit probabilities and speed profiles within the NTPs are shaped by these locations and times as well as the minimum time required to conduct such activity.

More generally, estimating the speed-related costs of an NTP can improve its functionality as a cost-benefit measure of individual space-time accessibility. Although this paper focuses on fuel consumption and CO_2 emissions, the general framework to estimate speed-related costs can be applied to other types of negative externalities. For instance, we can relate the estimated speed profiles to the distributions of traffic fatalities within a transportation network to reveal possible space-time correlations between them. We can also overlay the simulated distribution of emissions with the individuals' activity trajectories to model their exposure to air pollution.

The framework to estimate speed-related costs can also be modified for travel modes other than driving. For instance, we can define NTPs for buses restricted by time points (stops where the bus is required to be at a certain time), model visit probabilities and speed distributions within the bus routes, and support bus operation. We can also define NTPs for car-sharing services using trip start and end locations and times, and estimate potential activity space of users and the related fuel consumption. Overall, the methods in this paper provide multiple approaches to improve space-time accessibility measures for cost-benefit analysis in sustainable transportation planning.

Acknowledgement

The research in this paper is supported by the National Science Foundation – United States under grant no. BCS-1224102, "Measuring the Environmental Costs of Space–time Prisms in Sustainable Transportation Planning".

Reference

Ahn, K., 1998. Microscopic Fuel Consumption and Emission Modeling. Master Thesis. Virginia Polytechnic Institute and State University, Virginia, United States.
An, F., Ross, M., 1993. Model of fuel economy with applications to driving cycles and traffic management. Transp. Res. Rec. 1416, 105–114.
Aziz, H.M.A., Ukkusuri, S.V., 2012. Integration of environmental objectives in a system optimal dynamic traffic assignment model. Comput. Civ. Infrastruct. Eng. 27. http://dx.doi.org/10.1111/j.1467-8667.2012.00756.x.
Baker, M.A., 1994. Fuel Consumption and Emission Models for Evaluating Traffic Control and Route Guidance Strategies. Master Thesis. Queen's University, Kingston, Canada.
Banister, D., 2008. The sustainable mobility paradigm. Transp. Policy 15, 73–80. http://dx.doi.org/10.1016/j.tranpol.2007.10.005.
Barth, M., An, F., Norbeck, J., Ross, M., 1996. Modal emissions modeling: a physical approach. Transp. Res. Rec. 1520, 81–88. http://dx.doi.org/10.3141/1520-10.
Bhat, C.R., Koppelman, F.S., 1999. Activity-based modeling of travel demand. In: Handbook of Transportation Science. Springer, pp. 35–61.
Boisjoly, G., El-Geneidy, A., 2016. Daily fluctuations in transit and job availability: a comparative assessment of time-sensitive accessibility measures. J. Transp. Geogr. 52, 73–81. http://dx.doi.org/10.1016/j.jtrangeo.2016.03.004.
Buchanan, J.M., Stubblebine, W.C., 1962. Externality. In: Classic Papers in Natural Resource Economics. Springer, pp. 138–154.
Carlsson-Kanyama, A., Linden, A.L., 1999. Travel patterns and environmental effects now and in the future: implications of differences in energy consumption among socio-economic groups. Ecol. Econ. 30, 405–417. http://dx.doi.org/10.1016/S0921-8009(99)00006-3.
Cervero, R., 1996. Mixed land-uses and commuting: evidence from the American housing survey. Transp. Res. A Policy Pract. 30, 361–377. http://dx.doi.org/10.1016/0965-8564(95)00033-X.
Cetin, M., 2015. Using GIS analysis to assess urban green space in terms of accessibility: case study in Kutahya. Int. J. Sust. Dev. World 22 (5), 420–424.
Cetin, M., Sevik, H., 2016. Change of air quality in Kastamonu city in terms of particulate matter and CO_2 amount. Oxid. Commun. 39 (4), 3394–3401.
Chapman, L., 2007. Transport and climate change: a review. J. Transp. Geogr. 15, 354–367. http://dx.doi.org/10.1016/j.jtrangeo.2006.11.008.
Chen, L., Yang, H., 2012. Managing congestion and emissions in road networks with tolls and rebates. Transp. Res. B Methodol. 46, 933–948. http://dx.doi.org/10.1016/j.trb.2012.03.001.
Dickerson, A.E., Molnar, L.J., Eby, D.W., Adler, G., Bedard, M., Berg-Weger, M., Classen, S., Foley, D., Horowitz, A., Kerschner, H., Page, O., Silverstein, N.M., Staplin, L., Trujillo, L., 2007. Transportation and aging: a research agenda for advancing safe mobility. Gerontol. Soc. Am. 47, 578–590. http://dx.doi.org/10.1093/geront/47.5.578.
Downs, J.A., Horner, M.W., 2012. Probabilistic potential path trees for visualizing and analyzing vehicle tracking data. J. Transp. Geogr. 23, 72–80. http://dx.doi.org/10.1016/j.jtrangeo.2012.03.017.
Environmental Protection Agency (EPA), 2012. Assessing the emissions and fuel consumption impacts of intelligent transportation systems (ITS). BiblioGov 1–74.
Farber, S., Neutens, T., Miller, H.J., Li, X., 2013. The social interaction potential of metropolitan regions: a time-geographic measurement approach using joint accessibility. Ann. Assoc. Am. Geogr. 103, 483–504. http://dx.doi.org/10.1080/00045608.2012.689238.
Franco, V., Kousoulidou, M., Muntean, M., Ntziachristos, L., Hausberger, S., Dilara, P., 2013. Road vehicle emission factors development: a review. Atmos. Environ. 70, 84–97. http://dx.doi.org/10.1016/j.atmosenv.2013.01.006.
Frey, H.C., Liu, B., 2013. Development and evaluation of a simplified version of moves for coupling with a traffic simulation model. In: 92nd Annual Meeting of the Transportation Research Board, Washington, DC, pp. 13–17.
Geurs, K.T., van Wee, B., 2004. Accessibility evaluation of land-use and transport strategies: review and research directions. J. Transp. Geogr. 12, 127–140. http://dx.doi.org/10.1016/j.jtrangeo.2003.10.005.
Ghali, M.O., Smith, M.J., 1995. A model for the dynamic system optimum traffic assignment problem. Transp. Res. B 29, 155–170. http://dx.doi.org/10.1016/0191-2615(94)00024-T.
Glaeser, E.L., Kahn, M.E., 2010. The greenness of cities: carbon dioxide emissions and urban development. J. Urban Econ. 67, 404–418. http://dx.doi.org/10.1016/j.jue.2009.11.006.
Grote, M., Williams, I., Preston, J., Kemp, S., 2016. Including congestion effects in urban road traffic CO_2 emissions modelling: do local government authorities have the right options? Transp. Res. Part D: Transp. Environ. 43, 95–106. http://dx.doi.org/10.1016/j.trd.2015.12.010.
Hägerstraand, T., 1970. What about people in regional science? Pap. Reg. Sci. 24, 7–24.
Hansen, W.G., 1959. How accessibility shapes land use. J. Am. Inst. Plann. 25, 73–76. http://dx.doi.org/10.1080/01944365908978307.
Howard, R.A., 2007. Dynamic Probabilistic Systems, Volume II: Semi-Markov and Decision Processes, Volume 2 of Dover Books on Mathematics. Dover Publication.
Humphrey, N., 1996. Expanding metropolitan highways: implications for air quality and energy use. Transp. Res. Rec. 183 (No. HS-042 177).
Janic, M., 2007. Modelling the full costs of an intermodal and road freight transport network. Transp. Res. Part D: Transp. Environ. 12, 33–44. http://dx.doi.org/10.1016/j.trd.2006.10.004.
Johnson, N.L., Kotz, S., Balakrishnan, N., 1996. Continuous univariate distributions. Wiley New York, NY.
Kopits, E., Cropper, M., 2005. Traffic fatalities and economic growth. Accid. Anal. Prev. 37, 169–178. http://dx.doi.org/10.1016/j.aap.2004.04.006.
Kuijpers, B., Othman, W., 2009. Modeling uncertainty of moving objects on road networks via space–time prisms. Int. J. Geogr. Inf. Sci. 23, 1095–1117. http://dx.doi.org/10.1080/13658810802097485.
Kuijpers, B., Miller, H., Othman, W., 2011. Kinetic space-time prisms. In: Proc. 19th ACM SIGSPATIAL Int. Conf. Adv. Geogr. Inf. Syst, pp. 162–170. http://dx.doi.org/10.1145/2093973.2093996.
Kwan, M.-P., 1998. Space-time and integral measures of individual accessibility: a comparative analysis using a point-based framework. Geogr. Anal. 30, 191–216. http://dx.doi.org/10.1111/j.1538-4632.1998.tb00396.x.
Lenntorp, B., 1976. Paths in space-time environments: a time-geographic study of movement possibilities of individuals. Environ. Plan. A 9, 961–972.
Mauzerall, D.L., Sultan, B., Kim, N., Bradford, D.F., 2005. NOx emissions from large point sources: variability in ozone production, resulting health damages and economic costs. Atmos. Environ. 39, 2851–2866. http://dx.doi.org/10.1016/j.atmosenv.2004.12.041.
Miller, H.J., 1991. Modelling accessibility using space-time prism concepts within geographical information systems. Int. J. Geogr. Inf. Syst. 5, 287–301. http://dx.doi.org/10.1080/02693799108927856.
Miller, H.J., 1999. Measuring space-time accessibility benefits within transportation networks: basic theory and computational procedures. Geogr. Anal. 31, 187–212. http://dx.doi.org/10.1111/j.1538-4632.1999.tb00976.x.
Miller, H.J., 2005. Necessary space - time conditions for human interaction. Environ. Plann. B. Plann. Des. 32, 381–401. http://dx.doi.org/10.1068/b31154.
Murrel, D., 1980. Passenger Car Fuel Economy: EPA and Road: A Report to the Congress in Response to the National Energy Conservation Policy Act of 1978, Public Law 95-619, Title IV, Part 1, Section 404.
Rabl, A., Spadaro, J.V., Van Der Zwaan, B., 2005. Uncertainty of air pollution cost estimates: to what extent does it matter? Environ. Sci. Technol. 39, 399–408. http://dx.doi.org/10.1021/es049189v.
Rigby, M., Winter, S., Krüger, A., 2016. A continuous representation of ad hoc ridesharing potential. IEEE Trans. Intell. Transp. Syst. http://dx.doi.org/10.1109/TITS.2016.2527052.
Schafer, A., Victor, D.G., 2000. The future mobility of the world population. Transp. Res. A Policy Pract. 34, 171–205. http://dx.doi.org/10.1016/S0965-8564(98)00071-8.
Song, Y., Miller, H.J., 2014. Simulating visit probability distributions within planar space-time prisms. Int. J. Geogr. Inf. Sci. 28, 104–125. http://dx.doi.org/10.1080/13658816.2013.830308.
Song, Y., Miller, H.J., Zhou, X., Proffitt, D., 2016. Modeling visit probabilities within network-time prisms using Markov techniques. Geogr. Anal. 48, 18–42.
Szeto, W.Y., Jiang, Y., Wang, D.Z.W., Sumalee, A., 2015. A sustainable road network design problem with land use transportation interaction over time. Networks Spatial Economics 15, 791–822.
Tompkins, M., Bunch, D., Santini, D., Bradley, M., Vyas, A., Poyer, D., 1998. Determinants of alternative fuel vehicle choice in the continental United States. Transp. Res. Rec. J.

Transp. Res. Board 1641, 130–138. http://dx.doi.org/10.3141/1641-16.
Vallamsundar, S., Lin, J., Konduri, K., Zhou, X., Pendyala, R.M., 2016. A comprehensive modeling framework for transportation-induced population exposure assessment. Transp. Res. D Transp. Environ. 46. pp. 94–113.
Versichele, M., Neutens, T., Claeys Bouuaert, M., Van de Weghe, N., 2014. Time-geographic derivation of feasible co-presence opportunities from network-constrained episodic movement data. Trans. GIS 18, 687–703. http://dx.doi.org/10.1111/tgis.12050.
Widener, M.J., Farber, S., Neutens, T., Horner, M., 2015. Spatiotemporal accessibility to supermarkets using public transit: an interaction potential approach in Cincinnati, Ohio. J. Transp. Geogr. 42, 72–83. http://dx.doi.org/10.1016/j.jtrangeo.2014.11.004.
Winter, S., Yin, Z.-C., 2010. Directed movements in probabilistic time geography. Int. J. Geogr. Inf. Sci. 24, 1349–1365. http://dx.doi.org/10.1080/13658811003619150.
Winter, S., Yin, Z.C., 2011. The elements of probabilistic time geography. GeoInformatica 15, 417–434. http://dx.doi.org/10.1007/s10707-010-0108-1.
Xie, Z., Yan, J., 2008. Kernel density estimation of traffic accidents in a network space. Comput. Environ. Urban. Syst. 32, 396–406. http://dx.doi.org/10.1016/j.compenvurbsys.2008.05.001.
Yin, Y., Lawphongpanich, S., 2006. Internalizing emission externality on road networks. Transp. Res. Part D: Transp. Environ. 11, 292–301. http://dx.doi.org/10.1016/j.trd.2006.05.003.
Zhou, X., Tanvir, S., Lei, H., Taylor, J., Liu, B., Rouphail, N.M., Frey, H.C., 2015. Integrating a simplified emission estimation model and mesoscopic dynamic traffic simulator to efficiently evaluate emission impacts of traffic management strategies. Transp. Res. Part D: Transp. Environ. 37, 123–136. http://dx.doi.org/10.1016/j.trd.2015.04.013.